ELSEVIER

Earth and Planetary Science Letters 198 (2002) 275–288

EPSL

www.elsevier.com/locate/epsl

Basin migration caused by slow lithospheric extension

J.W. van Wijk *, S.A.P.L. Cloetingh

Faculty of Earth and Life Sciences, Vrije Universiteit, De Boelelaan 1085, 1081 HV Amsterdam, The Netherlands

Received 19 July 2001; received in revised form 15 February 2002; accepted 25 February 2002

Abstract

Sedimentary basin migration caused by low lithospheric extension rates is investigated using a two-dimensional dynamic numerical model of the lithosphere. We find that continental breakup will eventually occur when larger extension velocities are used. The duration of rifting prior to continental breakup is dependent on the extension velocity. Stretching the lithosphere with lower velocities does not lead to breakup. Instead, the locus of maximum extension migrates. Deformation localizes outside the first formed basin that is in turn uplifted. This basin then becomes a 'cold spot' in the area. In this case, syn-rift cooling predominates; the lithosphere regains its strength during stretching instead of becoming weaker, and the lithosphere necking zone becomes stronger than surrounding regions. The transition velocity is, for the cases studied, about 8 mm/yr, while the locus of maximum thinning migrates after about 50–60 Myr. A comparison with observations of the mid-Norwegian, Galicia and ancient South Alpine margins shows a close resemblance of important features.

Keywords: basins; migration; basin inversion; Voring Plateau; continental drift

1. Introduction

Numerous examples have been described in the literature of extensional regions in which the main locus of extension shifted in time (e.g. [1–4]). In these areas, typically several sedimentary basins are found that are closely located, with more or less the same orientation of the basin axes, and a time of formation often several tens of millions of years apart. The centers of lithosphere thinning in these areas seem to have migrated in time.

A well documented example of such an area is the mid-Norwegian passive continental margin. Prior to the final Late Cretaceous–Early Tertiary rifting event that led to continental breakup, the mid-Norwegian Vøring margin was affected by several rifting events ([1,3,5]). These resulted in the formation of several sedimentary basins positioned on the passive margin between the Norwegian mainland and the continent–ocean boundary (Fig. 1). On a basinwide scale the margin may be divided in the Permo-Triassic Trøndelag Platform, situated in the east, the Jurassic–Cretaceous Vøring Basin, in the center of the margin shelf, and a western extended zone related to the final stretching event that resulted in continental breakup at the Paleocene–Eocene transition [4,7,8], adjacent to the ocean–continent boundary. The Nordland Ridge and Vøring Marginal High are uplifted structures. Although there still exist thorough uncertainties on the deeper structures of the

* Corresponding author. Fax: +31-20-6462457.
E-mail address: wijk@geo.vu.nl (J.W. van Wijk).

0012-821X/02/$ – see front matter
PII: S0012-821X(02)00560-5

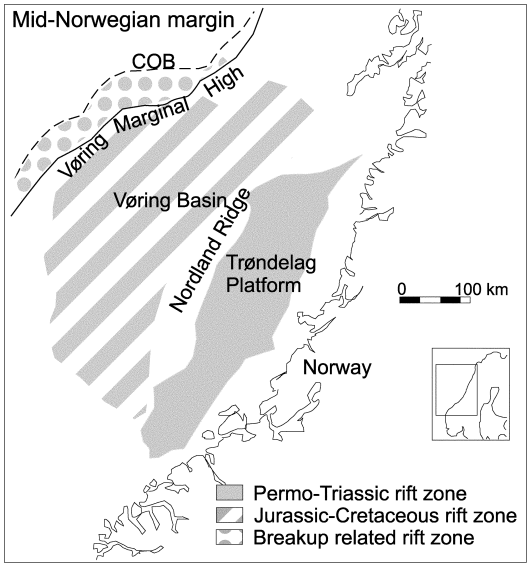

Fig. 1. Sketch of three rift zones of the mid-Norwegian margin (after [6]).

mid-Norwegian margin, and the affected width of the pre-Jurassic extension phase remains unclear [9], the locus of extension is often suggested to have shifted westward in time, from the Trøndelag platform to the Vøring margin to the margin edge (e.g. [3,4,7]).

Other areas where basin depocenter shift has been observed are the nonvolcanic Galicia margin and the passive rifted ancient South Alpine margin (e.g. [10,11]). On the Galicia margin the location of rifting shifted from the location of the Interior Basin towards the site of future breakup, on the South Alpine margin from the Lombardian Basin towards the future breakup location.

1.1. Hypotheses of rift migration

Several hypotheses exist on causes of rift migration, based on the principle that rifting occurs at locations where the lithosphere is weakest. A mechanism for limiting extension at one location has been studied by, for example, England [12], Houseman and England [13], and Sonder and England [14]. They found that cooling of the continental lithosphere during stretching might increase its strength, so that the locus of deformation may shift to a region of low strain [14]. With this mechanism, other influences like changes in plate boundary forces are not needed to explain observations of basin migration.

Migration of the locus of extension is frequently suggested to be the consequence of multiple stretching phases, with intermediate periods in which the lithosphere is not under tensile stress. Hereby, the weakened lithosphere resulting from the first stretching phase needs time to cool sufficiently and regain enough strength before the onset of the next stretching event. This explanation requires, therefore, a long period of tectonic quiescence between successive rifting events. It was shown by Bertotti et al. [11], in a model of the thermomechanical evolution of the South Alpine rifted margin, that the thinned parts of the margin could indeed be stronger than the rest of the margin. An explanation for this is that, after lithospheric thinning, the proportion of stronger mantle material vs. weaker crustal material is larger in comparison to non-thinned lithosphere [11]. This hypothesis goes together with a sudden time-dependent change in the magnitude of the intraplate stress field, causing the different stretching and non-stretching phases.

Steckler and Ten Brink [15] concluded, from considering lithospheric strength variations in the northern Red Sea region, that the strength of the lithosphere controls the locations of rifting and possibly new plate boundaries. For the northern Red Sea region this includes a shift in the location of maximum deformation during time. Strength variations in this area are influenced by several factors, like thickness and composition of the crust, sediment thickness, and geotherm. Sawyer and Harry [16] modeled rift migration in the USA Baltimore Canyon trough by including the asymmetry of the pre-rift geometry. Laterally offset pre-existing weaknesses in crust and upper mantle resulted, when the lithosphere was extended, in a shift of the rift location.

Manatschal and Bernoulli [10] found that rifting migrated during Galicia and ancient Adria margin formation in the direction of future breakup. They proposed that cooling and strengthening of the lithosphere during rifting forced a shift in the rift location to previously not or basely thinned areas. The process of syn-rift cooling

has also been proposed to explain the formation of some of the narrow–wide margin pairs of the South Atlantic [17] and basin migration on the ancient South Alpine passive rifted margin [11].

1.2. Migration by continuous slow lithospheric extension

In this study basin depocenter migration by continuous slow lithospheric extension is investigated. When the lithosphere is extending fast, the upwelling of warm mantle material in the area undergoing lithosphere necking is almost adiabatic. When the lithosphere is stretched with lower rates, syn-rift (lateral) cooling of the necking area will play a more important role. Intuitively, it can be reasoned that a set of conditions may exist where syn-rift cooling prevails. This would be the case when the lithosphere is stretched with progressively smaller rates. At some point, the lithosphere would regain its strength upon stretching rather than further losing it, and the necking zone could become stronger than its surrounding regions [12–14]. Hence, during continued stretching, migration of the necking area could be expected [14].

In this study, the lithosphere possessing an initially symmetric upper mantle weakness is extended in a visco-elastic plastic finite element model. When large extension velocities are used, focusing of deformation takes place, causing necking and eventually continental breakup. This will hereafter be referred to as 'standard' rifting. A different evolution of localization takes place when the lithosphere is extended with smaller velocities. In these cases, the necking area may start migrating, and hence, prevent continental breakup. The results of the modeling will be compared to observations of basin migration at the mid-Norwegian, Galicia and ancient South Alpine margins.

2. Modeling approach

To study lithosphere extension, a two-dimensional finite element model is used [18,19]. The program is based on a Lagrangian formulation, which makes it possible to track (material) boundaries, like the Moho, in time and space. A drawback of the Lagrangian method is that it is not suitable for solving very large grid deformation problems. This is a problem in analysis of extension of the lithosphere, which is often accompanied by large deformations. The elements might become too deformed to yield accurate or stable solutions. In order to overcome this problem the finite element grid is periodically remeshed.

2.1. Lithosphere deformation

In the numerical model the base of the lithosphere is defined by the 1300°C isotherm. Under such conditions, approximately the upper half of the thermal lithosphere behaves elastically on geological time scales, while in the lower half stresses are relaxed by viscous deformation. This visco-elastic behavior is well described by a Maxwell body [20], resulting in the following constitutive equation for a Maxwell visco-elastic material:

$$\dot{\varepsilon} = \frac{1}{2\mu}\sigma + \frac{1}{E}\frac{\mathrm{d}\sigma}{\mathrm{d}t} \tag{1}$$

in which $\dot{\varepsilon}$ is strain rate, μ is dynamic viscosity, σ is stress and E is Young's modulus [20]. For a Newtonian fluid the dynamic viscosity μ is constant. In the lithosphere, however, non-linear creep processes prevail [21,22], and the relation between stress and strain rate can be described by:

$$\dot{\varepsilon} = A\sigma^n \exp\frac{-Q}{RT} \tag{2}$$

where A, n and Q are experimentally derived material constants [21,22], n is the power law exponent, Q is activation energy, R is the gas constant and T is temperature.

The state of stress is constrained by the force balance:

$$\nabla\cdot\sigma + \rho g = 0 \tag{3}$$

where g is gravity and ρ is density.

In this model it is assumed that mass is conserved and the material is incompressible. The continuity equation following from the principle

of mass conservation for an incompressible medium is:

$$\nabla \vec{v} = 0 \tag{4}$$

In the model, the density is dependent on the temperature following a linear equation of state:

$$\rho = \rho_0(1-\alpha T) \tag{5}$$

where ρ_0 is the density at the surface, α is the thermal expansion coefficient and T is temperature.

Besides visco-elastic behavior, processes of fracture and plastic flow play an important role in deformation of the lithosphere. This deformation mechanism is active when deviatoric stresses reach a critical stress level. Here the Mohr–Coulomb criterion is used as a yield criterion to define the critical stress level. The Mohr–Coulomb strength criterion is defined as:

$$|\tau_n| \leq c - \sigma_n \tan \varphi \tag{6}$$

where τ_n is the shear stress component, σ_n is the normal stress component, c is the cohesion of the material and φ is the angle of internal friction [23]. Stresses are adjusted every time step when the criterion is reached. Frictional sliding and fault movement are not explicitly described by this criterion, analogous to [24].

The displacement field is obtained by solving Eqs. 1–6. We used 2560 straight-sided seven-node triangular elements, with a 13-point Gaussian integration scheme. As the time discretization schemes used are fully implicit, the system is unconditionally stable. However, the exactness of the solution remains dependent on the time step size, which is why the Courant criterion was implemented.

Processes like sedimentation and erosion are not incorporated in the modeling. They do affect the evolution of a rift basin and rift shoulders, and can change the strength of the lithosphere [25].

2.2. Thermal evolution

The temperature field in the lithosphere is calculated every time step using the heat flow equation:

$$\rho c_p \frac{dT}{dt} = \partial_j k \partial_j T + H \tag{7}$$

where the density ρ is defined by Eq. 5, c_p is specific heat, k is conductivity and H is crustal heat production. Temperatures are calculated on the same grid as the velocity field, and advection of heat is accounted for by the nodal displacements.

2.3. Configuration and initial and boundary conditions

The model domain is divided into an upper crust, a lower crust and a mantle lithosphere part (Fig. 2). The layers have been assigned different rheological parameters; a granite upper crust, diabase lower crust and olivine mantle were chosen [22]. The rheological parameters are listed in Table 1. In order to facilitate localization of deformation, the crust is thickened by 2 km in the center of the domain. The imposed Moho surface is assumed to be a linear feature parallel to the future basin axis. This dip in the Moho causes a local weakness in the upper mantle and locally reduces the lithospheric strength. Henk [24] describes rifting of a lithosphere with this configuration as postconvergent extension that occurs after thermal equilibration of the thickened crust. In the mid-Norwegian margin the Caledonian Or-

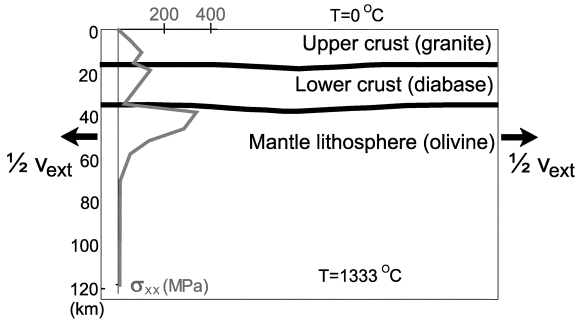

Fig. 2. Initial model configuration and horizontal deviatoric stress field. v_{ext} is extension velocity. Upon stretching of the lithosphere, the width of the model domain increases while its thickness decreases, preserving volume.

Table 1
Material parameter values

Parameter	Value
Density	2700 (u.c.), 2800 (l.c.), 3300 (m.l.) [kg/m^3]
Thermal expansion	1×10^{-5} [K^{-1}]
Crustal heat production	1×10^{-6} [W/m^3]
Specific heat	1050 [J/kg/K]
Conductivity	2.6 (crust), 3.1 (mantle) [W/m/K]
Bulk modulus	3.3×10^{10} (crust), 12.5×10^{10} (mantle) [Pa]
Shear modulus	2×10^{10} (crust), 6.3×10^{10} (mantle) [Pa]
Power law exponent n	3.3 (u.c.), 3.05 (l.c.), 3.0 (m.l.)
Activation energy Q	186.5 (u.c.), 276 (l.c.), 510 (m.l.) [kJ/mol]
Material constant A	3.16×10^{-26} (u.c.), 3.2×10^{-20} (l.c.), 7.0×10^{-14} (m.l.) [Pa^{-n}/s]
Friction angle	30°
Dilatation angle	0°
Cohesion factor	20×10^6 [Pa]
(Initial) thickness of model domain H	125 [km]

ogeny probably resulted in a crust that was thickened before the onset of rifting [5].

The model is not pre-stressed; deformation is driven by velocity boundary conditions. The right and left sides of the model domain are pulled with a constant velocity v (Fig. 2). This constant velocity boundary condition implies that the strain rate decreases with time, which is representative for basin-forming processes. The range of the constant extension rates tested is between ~3 and ~30 mm/yr. This falls within the range of present-day plate velocities as obtained by using the Global Positioning System [26]. The surface is unconstrained and on the base of the model a vertical velocity component is prescribed calculated from the principle of volume conservation.

Temperatures are calculated using the heat flow Eq. 7. The initial geotherm is in steady state. The temperature at the surface is 0°C, and at the base of the model (125 km depth) it is 1333°C. The heat flow through the right and left sides of the domain is zero. The crustal heat production is constant (Table 1).

3. Results

Several tests were performed in which the lithosphere was extended with different constant velocity boundary conditions ranging from rather large velocities of ~30 mm/yr to extension velocities of ~3 mm/yr. In these tests the model setup (see Fig. 2) is similar. The results suggest that two principally different patterns of development exist: when the lithosphere is extended with a total velocity less than ~8 mm/yr, localization of deformation evolves distinctly differently from when the lithosphere is stretched with higher rates.

To check the possibility that the horizontal size of the model domain might control any of the processes, some tests were performed with much larger horizontal model sizes as well. The horizontal size of the model domain proved to be of no influence on the results.

3.1. Rifting resulting in continental breakup

3.1.1. Evolution of lithosphere deformation

As the rift structures resulting from the larger boundary velocity models ('standard necking cases') do not differ significantly, one representative test in which the lithosphere was stretched with a total velocity of about 16 mm/yr is discussed here. When the lithosphere is extended, the deformation localizes in the center of the domain where the initial mantle weakness was introduced. Thinning of the crust and mantle lithosphere concentrates here, and mantle material starts to well up (Fig. 3). Thinning of the crust and mantle lithosphere continues, eventually resulting in continental breakup, after ~27 Myr of stretching. Continental breakup is here defined as occurring when the crust is thinned by a factor 20, but another factor or another definition for continental breakup could also have been chosen. This definition corresponds to about 40–50% of extension of the model domain at continental breakup. The thinning factors of the crust (β) and mantle (δ) parts of the lithosphere are shown in Fig. 4. The base of the mantle lithosphere is the 1300°C isotherm, and β and δ are defined to be the ratio between the initial and the present thick-

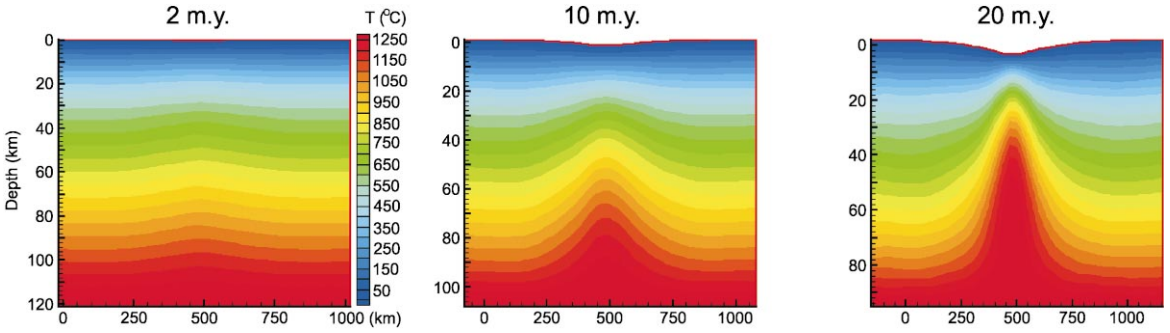

Fig. 3. Thermal evolution of lithosphere for case $v_{ext} \approx 16$ mm/yr, 2, 10 and 20 Myr after stretching started. Note the changing horizontal and vertical scales in the panels indicating the changing sizes of the model domain upon stretching.

ness of the crust or mantle lithosphere respectively.

The total (integrated) strength of the lithosphere during rifting is shown in Fig. 5. The center of the model domain where the initial mantle weakness was imposed is the weakest part; this continues to be so until breakup. The values of the integrated strength of continental lithosphere vary between 10^{12} and 10^{13} N/m, the higher values characterize Precambrian shields [21,27]. The strength of the lithosphere in the model falls within this range. The strength decreases with time, caused by thinning and heating of the lithosphere as a consequence of stretching, the non-linear rheology, and decreasing strain rates.

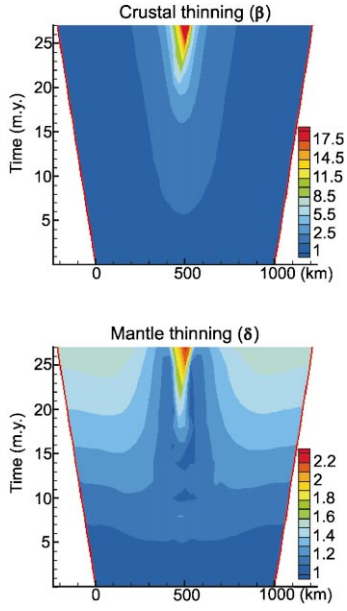

Fig. 4. Evolution of thinning factors of crust (β) and mantle lithosphere (δ) for case $v_{ext} \approx 16$ mm/yr. Breakup after ~ 27 Myr. Width of the model domain (horizontal axis) vs. time (vertical axis). The width of the model domain increases as the lithosphere is extended.

3.1.2. *Relation between rift duration and extension velocity*

The evolution of the localization of deformation in other cases with higher constant boundary velocities is comparable to that discussed above. One zone develops where deformation concentrates, and thinning continues, eventually resulting in continental breakup in all cases. The duration of rifting until the breakup depends on the extension velocity. When the lithosphere is stretched with larger velocities, it takes less time to reach continental breakup (Fig. 6). When the total extension velocity is less than ~ 8 mm/yr, stretching of the lithosphere does not lead to continental breakup. This is discussed in more detail

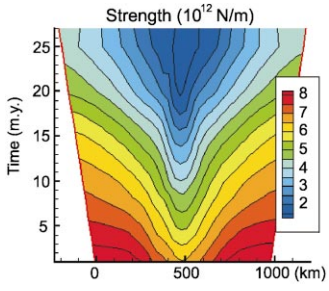

Fig. 5. Evolution of lithosphere strength ($\int_0^H \sigma(z)\,dz$), in N/m, for case $v_{ext} \approx 16$ mm/yr.

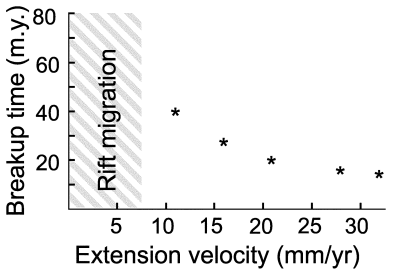

Fig. 6. Rift duration to continental breakup as a function of total extension velocity (stars). Rifting eventually results in breakup at larger extension rates, while at lower rates syntectonic cooling prevails and the rift migrates before breakup is reached (see text).

in Section 3.2. The dependence of rift duration on potential mantle temperature is discussed in Van Wijk et al. [28]. The shape of the rift shows no clear dependence on the velocity boundary condition tested here (see also Bassi [29]).

The tendency for the lithosphere to neck (or to focus strain) is weaker with decreasing extension velocity. When the stresses exerted on the lithosphere are smaller, the rate of localization is also slowed down. The mantle upwelling is slower and syn-rift lateral conductive cooling plays a more important role. When the lithosphere is stretched at high rates, the upwelling of mantle material is fast (almost adiabatic) with little or no horizontal heat conduction. The fast rise of hot material further reduces the strength of the lithosphere in the central region, with the consequence that deformation and thinning are even further accelerated. The result is a short rifting period and rapid continental breakup.

3.2. Rift migration

3.2.1. Thermal evolution

When extension is characterized by lower velocities, the lithosphere reacts differently. The results of one representative test (total extension rate of $\sim$6 mm/yr) have been selected to illustrate this. The lithosphere is stretched relatively slowly in this case for a period of more than 100 Myr. The thermal evolution of the lithosphere is shown in Fig. 7. During the first 30 Myr after onset of stretching, deformation localizes in the center of the domain where the lithosphere was initially weakened (Fig. 2). Mantle material wells up and a sedimentary basin is formed. Then, as lithospheric stretching proceeds, temperatures begin to decrease (see panels 45 Myr and 50 Myr; Fig. 7), in contrast to what happened in the standard necking case shown in Fig. 3. Development of the upwelling zone ceases and the lithosphere cools in the center of the domain. Cooling of the central zone continues, while after 70 Myr an increase in temperature is visible on both sides of the central zone. These new upwelling zones further develop (Fig. 7, 110 Myr panel) and two new basins are formed adjacent to the first basin. Temperatures in the lithosphere below the first-stage basin are now lower than temperatures in the surrounding lithosphere; a 'cold spot' is present in an area that previously underwent extension (see also Fig. 8). Surface heat flow values reflect this thermal structure; the surface heat flow values are lower in the first-stage basin (66 mW/m^2) than in the surrounding areas (75 mW/m^2) at 110 Myr.

3.2.2. Lithosphere thinning

The thinning factors of the crust and mantle lithosphere are shown in Fig. 8. Thinning of the crust starts in the central weakness zone of the domain, as expected. One basin is formed, with a maximum thinning factor of $\sim$1.85 for the crust. Crustal thinning in the central basin continues until about 65 Myr after the onset of stretching, at which time the locus of thinning shifts towards both sides of the first basin. The loci of maximum thinning of the new 'rifts' are at a distance of about 500 km from the center of the first rift. The first necking zone is not further thinned, although stretching of the lithosphere continues. Instead, two new basins have developed, below which further thinning of the lithosphere is accommodated. The thinning factor of the mantle lithosphere reflects this behavior. During the $\sim$45 Myr after stretching started the upwelling mantle material causes δ to be larger in the central zone of the domain than in its surroundings. After this time, however, temperatures decrease rapidly in this area (see also Fig. 7). New upwelling zones develop on both sides and δ decreases in the region of the first basin and increases where the new basins develop.

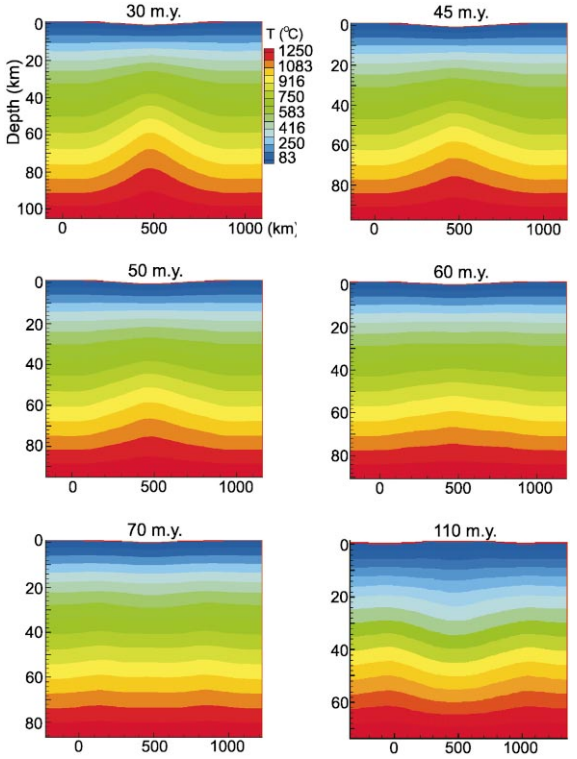

Fig. 7. Thermal evolution of lithosphere for migrating rift case, $v_{ext} \approx 6$ mm/yr, times in Myr after stretching started.

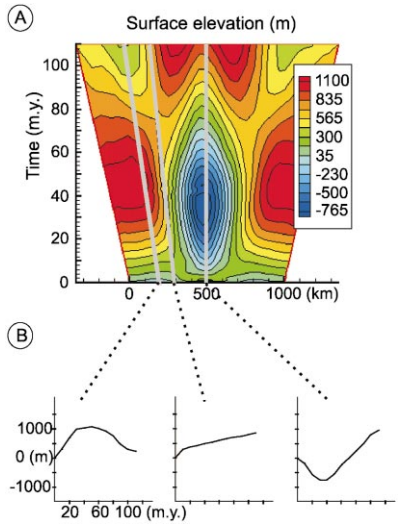

Fig. 9. (A) Evolution of relative surface topography for migrating rift case, $v_{ext} \approx 6$ mm/yr. Gray lines indicate the positions of the corresponding synthetic subsidence curves derived from this panel, shown in B. (B) Synthetic subsidence curves for three locations indicated in A: in the first-stage basin (right panel), outside this basin but in the new basin (left panel) and in the transition zone (middle panel).

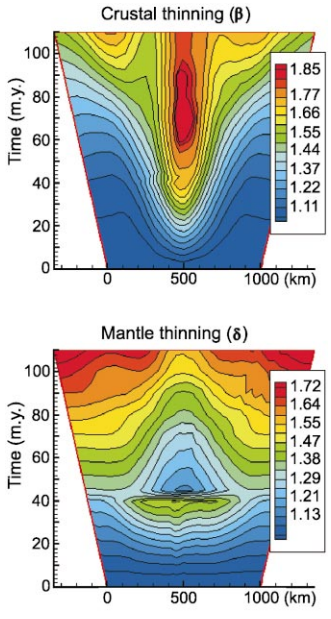

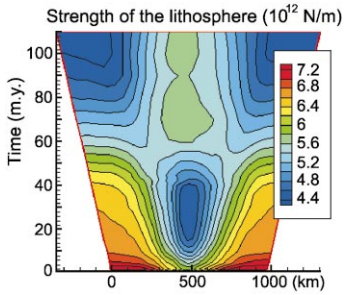

Fig. 10. Lithosphere strength evolution for migrating rift case, $v_{ext} \approx 6$ mm/yr.

←

Fig. 8. Evolution of thinning factors for crust (β) and mantle lithosphere (δ) for case $v_{ext} \approx 6$ mm/yr. No continental breakup. The asymmetry (upper panel) is caused by the asymmetry of the finite element grid that was used. We used triangular-shaped elements that resulted in a not perfectly symmetric mesh and initial Moho topography. The wiggles in the lines (lower panel, upper right) are due to interpolation inexactnesses while calculating the mantle thinning.

3.2.3. Tectonic subsidence

The relative topography of the surface and tectonic subsidence curves for three different locations are shown in Fig. 9. The central basin reaches a maximum depth of about 760 m. This tectonic subsidence would be further amplified by sedimentation. The basin is at its maximum depth ~35 Myr after stretching started. Then the basin subsidence commences and at both sides of the basin surface subsides. Ziegler [30] defined basin inversion as the reversal of the subsidence patterns of a sedimentary basin in response to compressional or transpressional stresses. Following this definition, no basin inversion takes place here as the lithosphere remains in a tensional regime. The synthetic tectonic subsidence curve for this basin (right panel) shows a clear reversal of the subsidence pattern. Here, basin uplift thus takes place in a stretching regime. The relative uplift is considerable; with values, depending on the location in the basin, of approximately 800–1700 m. The left panel in Fig. 9B shows the subsidence curve at the location of the migrated rift. After about 50 Myr subsidence starts. The central panel shows the subsidence curve for the 'transition zone' between the original basin and the basin formed after migration. This area displays continuous uplift.

3.2.4. Lithosphere strength

The total strength of the lithosphere, obtained by integrating the stress field over the thickness of the lithosphere [21], is shown in Fig. 10. The central part of the model domain is weaker than elsewhere until about 55 Myr after stretching started. Its minimum strength value is already reached by 30 Myr. Thereafter the strength increases, but remains less than for the rest of the domain. From 55 Myr, the smallest values of lithospheric strength are found on both sides of the central basin. By comparing the strength with the thermal structure of the lithosphere (Fig. 7), the strong dependence of the strength on the temperature is easily demonstrated.

3.2.5. Lithosphere deformation

The horizontal and vertical components of the velocity field are shown in Fig. 11, for several time intervals. These were corrected for the kinematic velocity field. In the first panels, from 25 Myr after stretching started, one strong central upwelling zone is present (see the vertical z component of the velocity field) with two weaker downwelling zones on either side. Material for the upwelling zone is drawn into the zone from deep in the lithosphere; in the horizontal or x component velocity panel it is visible that mantle material moves towards the left on the right side of the center and towards the right on the left side of the center, so the movement of the material is towards the center, deep in the lithosphere. The thickness of this horizontal convergence zone is about 20 km.

By 50 Myr after stretching started, the upwelling zone becomes split into two zones. While the lithosphere is still extending with the same velocity, the maximum velocities in the horizontal and vertical direction become reduced by almost one order of magnitude. Mantle material still wells up, but the upwelling is considerably weaker. After 60 Myr two separate, new upwelling zones are active, and the upwelling region has been reversed to form a downwelling zone. In the horizontal velocity component panel a similar split is visible; two converging zones have developed. By 110 Myr the two upwelling zones are fully developed, and the horizontal and vertical velocities are once again increasing. The x component of the velocity field shows that the first-stage basin that was formed is eventually uplifted with respect to its surroundings; as part of the two upwelling systems, crustal and mantle material converges in the area of former basin formation. The response of the lithosphere to other low extension velocities is similar to the case described above. The single upwelling system eventually splits into two new upwelling zones. The first-stage basin is uplifted and two separate, new rifts are formed.

3.2.6. Sequence of events

Comparing Figs. 7, 10 and 11, we observe that the strength in the center of the domain already starts to increase (at 35 Myr), while the upwelling zone does not split into two zones until ~50 Myr after stretching began. Temperatures in the upwelling area start to drop from 35 Myr, which

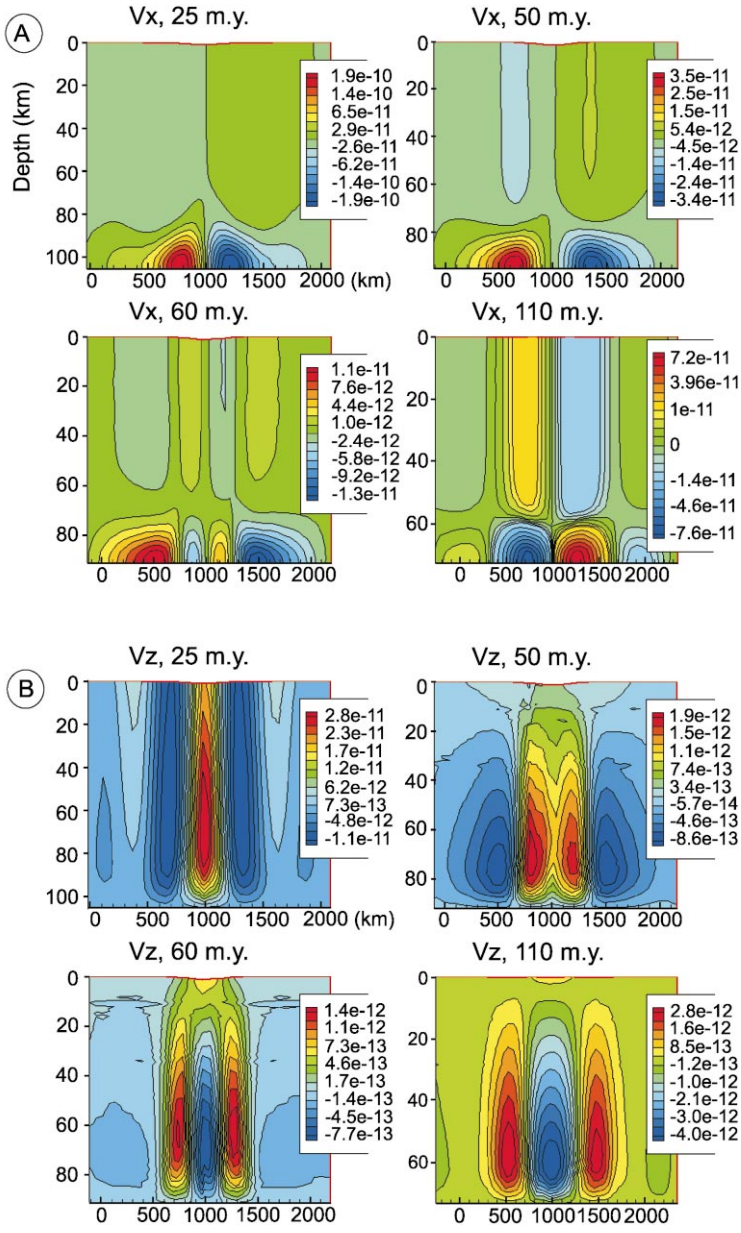

Fig. 11. Corrected velocity field (see text) in the lithosphere at 25, 50, 60 and 110 Myr after stretching began, for migrating rift case, $v_{ext} \approx 6$ mm/yr. (A) Horizontal component of the velocity field. Velocities are positive to the right, negative to the left. (B) Vertical component of the velocity field. Velocities are positive upwards, negative downwards. Velocities in m/s. 1e-10 means 1×10^{-10}. Note that a larger part of the model domain is shown here than in the other figures for a better illustration.

initiates the re-strengthening of the thinned lithosphere. Considerable syn-rift conductive cooling of the warm upwelling mantle material seems to cause this reduction in temperature. The upwelling is so slow that syn-rift cooling can play a major role. The strength of the lithosphere, however, attains its minimum value in the center part of the domain until the upwelling zone has begun

to split up, and crustal thinning in this region continues until ~60 Myr. Renewed crustal thinning on both sides of the first basin is delayed for ~20 Myr. It starts when the two new upwelling systems have fully developed.

3.3. Multiple rifts

In the model, rifting in the original basin is taken over by rifting in two new zones. This is the case in an almost perfectly symmetric lithosphere configuration. In the Earth however, such perfectly symmetric situations are very unlikely (e.g. because of pre-existing structural inhomogeneities, deep crustal structures, etc.). Therefore, renewed rifting is likely to take place at one preferred side of the original basin.

When the rate at which the lithosphere is extended is larger than a certain 'critical' value, extension may eventually end in continental breakup. Smaller extension rates will not result in breakup, instead, when extension continues, the locus of maximum extension shifts, the old basin is abandoned and rifting concentrates in other areas. This may lead to a region of lithosphere extension with several rifts. The basin that is formed first is (partly) uplifted while the next basin is formed. This cycle can be repeated one or several times, resulting in, for example, a third basin. Between the cessation of rifting in the first-stage basin and the onset of rifting in the second-stage basin a period of some tens of millions of years is predicted with the setup and rheological parameters used. The rifts may almost border on one another; a small zone without significant subsidence or uplift and an inverted or uplifted region separate the basins. The critical extension rate which separates the two localization modes (resulting in continental breakup and resulting in rift migration) is about 8 mm/yr. The dependence of these parameters on initial and rheological conditions, however, needs further investigation.

While in the modeling the lithosphere undergoes constant extension, separate periods of localized deformation or necking can be distinguished. From the final situation alone it is difficult to determine whether the area of lithosphere extension with multiple rift zones is the result of one stretching episode or multiple stretching phases. In order to generate rift migration, sudden changes in the intra-plate stress field are not required, provided that the rate at which the lithosphere is extended is low.

The results of this study are qualitatively in agreement with previous studies on limited extension (e.g. [12–14]). Sonder and England [14] found that just after the onset of extension the strength of the lithosphere decreases slightly, while after some time cooling increases the strength. Breakup is expected at high strain rates, the locus of deformation shifts at lower strain rates. The transition is predicted between strain rates of 10^{-14} and 10^{-16} s^{-1}. England [12] found that the duration of rifting until breakup is probably less than 10–20 Myr, our modeling study predicts that longer rift durations are possible. Houseman and England [13] predicted that the maximum extension factor before extension ceases is probably <1.5; we find slightly larger values before migration takes place ($\beta \approx 1.85$). Shifting of the location of extension is also found in modeling studies by Bassi [29,31], Bassi et al. [32] and Hopper and Buck [33], on smaller scales and time spans.

4. Comparison with observations of migrating rifts

In the mid-Norwegian margin, three rift zones are present (see Fig. 1); these formed during a Permo-Triassic episode (290–235 Ma), a Late Jurassic–Early Cretaceous episode (170–95 Ma) and a Late Cretaceous–Early Tertiary episode (75–57 Ma) [3,5,7], respectively, all under E–W to SE–NW directed extension [9]. The time gap between the successive rifting events was ~20–60 Myr. Maximum crustal thinning factors range from 1.6 for the Permo-Triassic Trøndelag Platform, to about 2.6 for the Late Jurassic–Early Cretaceous Vøring Basin [6]. In comparison with the modeling results, the time gap between the successive rifting events is of the same order, and the crustal thinning factors also correspond favorably.

The model experiments predict an uplift of (part of) the first-stage basin, and re-thickening of the thinned crust. On the mid-Norwegian mar-

gin both the Nordland Ridge and the Vøring Marginal High are uplifted structures, as well as the western part of the Vøring Basin (Fenris Graben, Hel Graben and Fulla Ridge) and the western part of the Trøndelag Platform [5]. The Nordland Ridge and western part of the Trøndelag Platform experienced uplift probably in the Early Cretaceous [5,8]. This uplift is suggested to be rift-flank uplift from the Vøring Basin formation [5]. The Vøring Marginal High and the western part of the Vøring Basin experienced regional uplift probably in the Early Tertiary [5]. This uplift is frequently suggested to be related to the thermal (or magmatic underplating) influence of the Iceland mantle plume during continental breakup (e.g. [34,35]). The observed inversions and uplifts are considerable; maximum estimations range from 1500 (Nordland Ridge) to 2400 m (Vøring Marginal High). The modeling predicts uplift, starting at the end of the formation of the first-stage basin and continuing during the first part of the formation of the second-stage basin. These pre-breakup uplifted structures of the mid-Norwegian margin may have experienced basin shift-related uplift. Other pre-breakup contractional structures at the Norwegian continental shelf have been suggested to be related to the Alpine Orogeny [36].

On both the Galicia and South Alpine margins, rifting migrated after about 20–30 Myr of extension to the location of eventual seafloor spreading. The Interior and Lombardian basins attained crustal thinning factors of about 1.4–1.5 [10,11,37], before the basins migrated. These extension factors and rift durations are smaller than the modeling predictions. On the Galicia margin, extension of the new (second-stage) basin was contemporaneous with uplift continentward (the Galicia Bank) [10], and Manatschal and Bernoulli [10] suggested that this might be a breakup-related isostatic edge effect. The similarity with the model-predicted uplift suggests that it is possibly basin migration related. Below the Lombardian basin, cooling started soon after the onset of rifting [38]. This is in agreement with the modeling results. The modeling results confirm the explanations of basin depocenter shifts on these margins by [10,11], who found that syn-rift cooling of the lithosphere led to strengthening, which eventually forced the locus of thinning to migrate to weaker and less extended areas.

The importance of understanding the interplay between extensional basins and inversion tectonics and uplifted structures has been addressed by Cloetingh et al. [39]. This study shows that these features, which are often related to compressional regimes, may also occur in extensional regimes.

5. Conclusions

This modeling study predicts that basin migration can be the result of constant stretching of the lithosphere with low rates. As the lithosphere is extended at progressively high rates, continental breakup eventually occurs. The duration of rifting prior to continental breakup is dependent upon the extension velocity; the larger the extension velocity, the sooner continental breakup will occur. When the lithosphere is stretched with a velocity lower than a 'critical' velocity, continuing stretching will eventually no longer result in continental breakup. Instead, syn-rift cooling starts to play a major role causing the originally developed necking zone to cease and new necking zones to develop. Deformation then localizes outside the first formed basin that is, in addition, uplifted. This basin becomes a 'cold spot' in the area. A qualitative comparison with observations of the mid-Norwegian, Galicia and ancient South Alpine passive continental margins shows a close resemblance of important features. Particularly interesting are the observed uplifted structures; they are predicted by the modeling as well. Another outcome of this modeling study is that one lithospheric extension episode appears to be sufficient to explain separate rift locations and episodes present in a single extensional area. Slow lithospheric extension appears to be a possible cause for basin migration.

Acknowledgements

We would like to thank W.R. Buck and R.H. Gabrielsen for very useful reviews and suggestions, and R. Stephenson for improving the Eng-

lish and the style of the manuscript. G. Bertotti, R. van der Meer and M. ter Voorde are thanked for discussions and suggestions, and R. Huismans and Y. Podladchikov for their large contribution to the numerical code. This is Publication 20010704 of the Netherlands Research School of Sedimentary Geology.*[AC]*

References

[1] P. Ziegler (Ed.), Evolution of the Arctic-North Atlantic and the western Tethys, Am. Assoc. Petrol. Geol. Mem. 43, 1988.

[2] P. Ziegler, Geodynamic processes governing development of rifted basins, in: F. Roure, N. Ellouz, V.S. Shein, I.I. Skvortsov (Eds.), Geodynamic Evolution of Sedimentary Basins, International Symposium Moscow, 1994, pp. 19–67.

[3] C. Bukovics, P.A. Ziegler, Tectonic development of the Mid-Norway continental margin, Mar. Petrol. Geol. 2 (1985) 2–22.

[4] E.R. Lundin, A.G. Doré, A tectonic model for the Norwegian passive margin with implications for the NE Atlantic: Early Cretaceous to break-up, J. Geol. Soc. London 154 (1997) 545–550.

[5] J. Skogseid, T. Pedersen, V.B. Larsen, Vøring Basin: subsidence and tectonic evolution, in: R.M. Larsen, H. Brekke, B.T. Larsen, E. Talleraas (Eds.), Structural and Tectonic Modelling and Its Application to Petroleum Geology, NPF Spec. Publ. 1, Elsevier, Amsterdam, 1992, pp. 55–82.

[6] J. Skogseid, O. Eldholm, Rifted continental margin off mid-Norway, in: E. Banda et al. (Eds.), Rifted Ocean-Continent Boundaries, Kluwer Academic, Dordrecht, 1995, pp. 147–153.

[7] P. Reemst, S. Cloetingh, Polyphase rift evolution of the Vøring margin (mid-Norway): constraints from forward tectonostratigraphic modeling, Tectonics 19 (2000) 225–240.

[8] J. Skogseid, S. Planke, J.I. Faleide, T. Pedersen, O. Eldholm, F. Neverdal, NE Atlantic continental rifting and volcanic margin formation, Geol. Soc. Spec. Publ. 167 (2000) 295–326.

[9] R.H. Gabrielsen, T. Odinsen, I. Grunnaleite, Structuring of the Northern Viking Graben and the Møre Basin; the influence of basement structural grain, and the particular role of the Møre-Trøndelag Fault Complex, Mar. Petrol. Geol. 16 (1999) 443–465.

[10] G. Manatschal, D. Bernoulli, Architecture and tectonic evolution of nonvolcanic margins: present-day Galicia and ancient Adria, Tectonics 18 (1999) 1099–1119.

[11] G. Bertotti, M. ter Voorde, S. Cloetingh, V. Picotti, Thermomechanical evolution of the South Alpine rifted margin (North Italy): constraints on the strength of passive continental margins, Earth Planet. Sci. Lett. 146 (1997) 181–193.

[12] P. England, Constraints on extension of continental lithosphere, J. Geophys. Res. 88 (1983) 1145–1152.

[13] G. Houseman, P. England, A dynamical model for lithosphere extension and sedimentary basin formation, J. Geophys. Res. 91 (1986) 719–729.

[14] L.J. Sonder, P.C. England, Effects of a temperature-dependent rheology on large-scale continental extension, J. Geophys. Res. 94 (1989) 7603–7619.

[15] M.S. Steckler, U.S. TenBrink, Lithospheric strength variations as a control on new plate boundaries: examples from the northern Red Sea region, Earth Planet. Sci. Lett. 79 (1986) 120–132.

[16] D.S. Sawyer, D.L. Harry, Dynamic modeling of divergent margin formation: application to the US Atlantic margin, in: A.W. Meyer, T.A. Davies, S.W. Wise (Eds.), Evolution of Mesozoic and Cenozoic Continental Margins, Mar. Geol. 102 (1991) 29–42.

[17] I. Davison, Wide and narrow margins of the Brazilian South Atlantic, J. Geol. Soc. London 154 (1997) 471–476.

[18] R.S. Huismans, Y.Y. Podladchikov, S.A.P.L. Cloetingh, Transition from passive to active rifting: relative importance of asthenospheric doming and passive extension of the lithosphere, J. Geophys. Res. 106 (2001) 11271–11291.

[19] A. Poliakov, Y.Y. Podladchikov, Diapirism and topography, Geophys. J. Int. 109 (1992) 553–564.

[20] D.L. Turcotte, G. Schubert, Geodynamics: Applications of Continuum Physics to Geological Problems, Wiley, New York, 1982, 450 pp.

[21] G. Ranalli, Rheology of the Earth, 2nd edn., Chapman and Hall, London, 1995, 413 pp.

[22] N.L. Carter, M.C. Tsenn, Flow properties of continental lithosphere, Tectonophysics 136 (1987) 27–63.

[23] P.A. Vermeer, R. de Borst, Non-associated plasticity for soils, concrete and rock, Heron 29 (1984) 3–64.

[24] A. Henk, Did the Variscides collapse or were they torn apart? a quantitative evaluation of the driving forces for postconvergent extension in central Europe, Tectonics 18 (1999) 774–792.

[25] E. Burov, S.A.P.L. Cloetingh, Erosion and rift dynamics: new thermomechanical aspects of post-rift evolution of extensional basins, Earth Planet. Sci. Lett. 150 (1997) 7–26.

[26] D.F. Argus, M.B. Heflin, Plate motion and crustal deformation estimated with geodetic data from the Global Positioning System, Geophys. Res. Lett. 22 (1995) 1973–1976.

[27] P. England, Comment on 'Brittle failure in the upper mantle during extension of the continental lithosphere' by D.W. Sawyer, J. Geophys. Res. 91 (1986) 10487–10490.

[28] J.W. Van Wijk, R.S. Huismans, M. ter Voorde, S.A.P.L. Cloetingh, Melt generation at volcanic continental mar-

gins: no need for a mantle plume?, Geophys. Res. Lett. 28 (2001) 3995–3998.
[29] G. Bassi, Factors controlling the style of continental rifting: insights from numerical modelling, Earth Planet. Sci. Lett. 105 (1991) 430–452.
[30] P.A. Ziegler, Compressional intra-plate deformations in the Alpine foreland – an introduction, Tectonophysics 137 (1987) 1–5.
[31] G. Bassi, Relative importance of strain rate and rheology for the mode of continental extension, Geophys. J. Int. 122 (1995) 195–210.
[32] G. Bassi, C.E. Keen, P. Potter, Contrasting styles of rifting: models and examples from the Eastern Canadian margin, Tectonics 12 (1993) 639–655.
[33] J.R. Hopper, W.R. Buck, The effect of lower crustal flow on continental extension and passive margin formation, J. Geophys. Res. 101 (1996) 20175–20194.
[34] O. Eldholm, J. Thiede, E. Taylor, Evolution of the Vøring volcanic margin, in: O. Eldholm, J. Thiede, E. Taylor et al. (Eds.), Proc. ODP Sci. Results 104 (1989) 1033–1065.
[35] J. Skogseid, T. Pedersen, O. Eldholm, B.T. Larsen, Tectonism and magmatism during NE Atlantic continental break-up: the Vøring margin, in: B.C. Storey, T. Alabaster, R.J. Plankhurst (Eds.), Magmatism and the Causes of Continental Break-up. Geol. Soc. London Spec. Publ. 68 (1992) 305–320.
[36] E. Vågnes, R.H. Gabrielsen, P. Haremo, Late Cretaceous-Cenozoic intraplate contractional deformation at the Norwegian continental shelf: timing, magnitude and regional implications, Tectonophysics 300 (1998) 29–46.
[37] G. Bertotti, V. Picotti, D. Bernoulli, A. Castellarin, From rifting to drifting: tectonic evolution of the south-Alpine upper crust from the Triassic to the Early Cretaceous, Sediment. Geol. 86 (1993) 53–76.
[38] C.A.E. Sanders, G. Bertotti, S. Tommasini, G.R. Davies, J.R. Wijbrans, Triassic pegmatites in the Mesozoic middle crust of the southern Alps (Italy): Fluid inclusions, radiometric dating and tectonic implications, Ecl. Geol. Helv. 89 (1996) 505–525.
[39] S.A.P.L. Cloetingh, Z. Ben-Avraham, W. Sassi, F. Horvath, Dynamics of basin formation and strike-slip tectonics, Tectonophysics 266 (1996) 1–10.